Title

The fingerprint of antimitochondrial antibodies and the etiology of primary biliary cholangitis

Journal

Hepatology, 65(5)

ISSN

0270-9139

Authors

Shuai, Zongwen

Wang, Jinjun

Badamagunta, Madhu

et al.

Publication Date

2017-05-01

DOI

10.1002/hep.29059

Peer reviewed

HHS Public Access

Author manuscript

Hepatology. Author manuscript; available in PMC 2018 May 01.

Published in final edited form as:

Hepatology. 2017 May ; 65(5): 1670–1682. doi:10.1002/hep.29059.

The Fingerprint of Antimitochondrial Antibodies and the Etiology of Primary Biliary Cholangitis

Zongwen Shuai[1,2], **Jinjun Wang**[1], **Madhu Badamagunta**[3], **Jinjung Choi**[1], **Guoxiang Yang**[1], **Weici Zhang**[1], **Thomas P. Kenny**[1], **Kathryn Guggenheim**[4], **Mark J. Kurth**[4], **Aftab A. Ansari**[5], **John Voss**[3], **Ross L Coppel**[6], **Pietro Invernizzi**[7], **Patrick S.C. Leung**[1], and **M. Eric Gershwin**[1]

[1]Division of Rheumatology/Allergy and Clinical Immunology, University of California Davis School of Medicine, Davis California USA

[2]Department of Rheumatology and Immunology, The First Affiliated Hospital of Anhui Medical University, Hefei 230022, China

[3]Department of Molecular Medicine, University of California Davis School of Medicine, Davis, California, USA

[4]Department of Chemistry, University of California Davis School of Medicine, Davis California, USA

[5]Department of Pathology, Emory University School of Medicine, Atlanta, Georgia, USA

[6]Department of Microbiology, Nursing and Health Sciences, Monash University, Clayton, Victoria, Australia

[7]Section of Digestive Diseases, International Center for Digestive Health, Department of Medicine and Surgery, University of Milan-Bicocca, Monza, Italy

Abstract

The identification of environmental factors that lead to loss of tolerance has been coined the Holy Grail of autoimmunity. Our work has focused on the reactivity of antimitochondrial autoantibodies (AMA) to chemical xenobiotics and has hypothesized that a modified peptide within PDC-E2, the major mitochondrial autoantigen, will have been immunologically recognized at the time of loss of tolerance. Herein we successfully applied intein technology to construct a PDC-E2 protein fragment containing amino acid residues 177–314 of PDC-E2 by joining a recombinant peptide spanning residues 177 to 252 (PDC-228) with a 62 residue synthetic peptide from 253 to 314 (PP), which encompasses PDC-E2 ILD. We named this intein-constructed fragment PPL. Importantly, PPL, as well as lipoic acid conjugated PPL (LA-PPL) and xenobiotic 2-octynoic acid conjugated PPL (2OA-PPL), are recognized by AMA. Of great importance, AMA has specificity for the 2OA modified PDC-E2 ILD peptide backbone distinct from antibodies that react with native lipoylated PDC-E2 peptide. Interestingly, this unique AMA subfraction is of the IgM isotype and more dominant in early stage PBC, suggesting that exposure to 2OA-PPL-like compounds occurs early in the generation of AMA. To understand the structural basis of this differential recognition we

Correspondence to: M. Eric Gershwin (megershwin@ucdavis.edu) or Patrick S.C. Leung (psleung@ucdavis.edu), Division of Rheumatology, Allergy and Clinical Immunology, University of California Davis School of Medicine, Davis CA 95616 USA.

analyzed PPL, LA-PPL and 2OA-PPL using electron paramagnetic resonance spectroscopy, with confirmations by ELISA, immunoblotting and affinity antibody analysis. We demonstrate that the conformation of PDC-E2 ILD is altered when conjugated with 2OA, compared to conjugation with lipoic acid. In conclusion a molecular understanding of the conformation of xenobiotic modified PDC-E2 is critical for understanding xenobiotic modification and loss of tolerance in PBC with widespread implications for a role of environmental chemicals in the induction of autoimmunity.

Keywords

Antimitochondrial antibodies; electron paramagnetic resonance spectroscopy; E2 subunit of the pyruvate dehydrogenase; inner lipoyl domain; intein mediated ligation; primary biliary cholangitis; xenobiotics; 2-octynoic acid

INTRODUCTION

The presence of anti-mitochondrial autoantibodies (AMA) is widely utilized for the diagnosis of primary biliary cholangitis (PBC) (1, 2). AMA can be detected before the appearance of disease symptoms. Although AMA is not associated with disease severity/prognosis (3), its presence before the development of liver pathology raises the possibility that it may contain information about early events in PBC. AMA recognize a unique conformational epitope within the inner lipoyl domain (ILD) of PDC-E2 (amino acid residue 177–314) (2) and we have hypothesized that the loss of tolerance to PDC-E2 is a result of chemical modification of this epitope following xenobiotic exposure (4). In fact, quantitative structure-activity relationship analysis demonstrated that when the lipoyl domain of PDC-E2 is modified with specific synthetic lipoyl mimics, some of the ensuing structures are recognized by AMA - often at levels higher than native PDC-E2 (5–7). Furthermore, AMA can be induced in animals immunized with a lipoyl mimic xenobiotic conjugated with bovine serum albumin (BSA) (8, 9). Fine analysis of AMA specificity demonstrates that AMA positive PBC sera contain subpopulations that recognize xenobiotic conjugated PDC-E2 ILD, native PDC-E2 peptide backbone and also the xenobiotic itself (4, 10). More interestingly, antibodies directed against xenobiotic conjugated PDC-E2 lipoyl domain are predominantly of the IgM isotype and are found in sera from early stage PBC patients (4, 10). These observations suggest that antibody specificity to xenobiotics may be footprints to the early events in loss of tolerance.

We have employed a novel protein engineering approach using intein technology to generate a 138 residue PDC-E2 fragment by ligation of a recombinant peptide encoding residues 177–252 of human PDC-E2 (PDC-228) to a 62 amino acid peptide (PP) corresponding to residues 253–314 of the ILD of human PDC-E2, of which the sole lysine residue of the PP was left unconjugated (control) or conjugated with either lipoic acid (LA) or 2-octynoic acid (2OA). This moiety, 2OA, was selected because AMA contain a population of antibodies that recognize the 2OA-PDC-E2 peptide that are demonstrably distinct from antibodies in the same AMA population that recognize the naturally lipoylated form of PDC-E2. These findings imply that when 2OA modifies the PDC-E2 peptide, it acquires a molecular

structure distinct from the naturally lipoylated form of the PDC-E2 peptide. The importance of our focus on 2OA is highlighted by the finding that 2OA is widely used in human products such as artificial flavorings, perfumes, soaps, detergents, lipsticks, toilet waters, facial creams, and perfumed cosmetics (5).

We set out to determine whether xenobiotic modification of the PDC-E2 lipoyl domain also leads to conformational changes to the PDC-E2 peptide backbone. The effect of the hapten conjugation on PDC-E2 structure was analyzed by electron paramagnetic resonance (EPR) spectroscopy, enzyme linked immunosorbent assay (ELISA), inhibition ELISA, immunoblotting and affinity antibody analysis. Our data indicate that 2OA-modified PDC-E2 exhibits a conformational change in the PDC-E2 ILD backbone, which is distinctly different from the native ILD of PDC-E2. Taken together, these observations provide key evidence for a chemical xenobiotic etiology of PBC.

MATERIALS AND METHODS

Serum samples

Serum samples from 128 patients with PBC, 37 patients with primary sclerosing cholangitis (PSC) and 52 healthy controls (HC) were used in this study. The clinical diagnosis of all patients was verified using published criteria (11–14). This study was approved by the Institutional Review Board of the University of California at Davis.

Construction, expression and purification of recombinant PDC-228

Recombinant PDC-228 was constructed in expression plasmid vector pTXB1. A 228 base pair insert encoding for amino acid residues 177 to 252 of PDC-E2 was amplified using oligonucleotide primers and ultimately the PCR product purified, The double digested PCR product and vector were finally purified and ligated and transformed into *E. coli* T7 Express Competent cells. Plasmid DNA from transformed *E. coli* colonies were verified by nucleotide sequence determination. Recombinant peptide was purified from an expression clone of PDC-228 in *E. coli* DH5 alpha and concentrated by ultrafiltration and quantified before subsequent IPL.

Preparation of the inner lipoyl domain (ILD) of human PDC-E2 by intein-mediated protein ligation (IPL)

Since there were five lysine residues (Lys177, Lys240, Lys241, Lys245 and Lys259) within the ILD of PDC-E2 (residues 177–314), we have employed intein-mediated protein ligation to obtain conjugates of 2OA and LA specifically at Lys259, as other lysine modifications on recombinant PDC-E2 (residues 177–314) would influence its molecular conformation. By employing a novel ligation approach, we have circumvented this difficulty by incorporating PP (residues 253–314) with its single lysine (Lys259) conjugated with 2OA or LA chemically. Subsequently it was ligated with the recombinant PDC-228 (residues 177–252), with its 4 native lysines unmodified. Firstly, a 62 aa peptide encoding residues 253–314 from the ILD of human PDC-E2 was chemically synthesized. This peptide contains a unique lysine residue for chemical conjugation of N-Hydroxysuccinimide (NHS)-activated xenobiotics and two cysteine residues (positions 253 and 273) around the lipoyl lysine to

facilitate subsequent EPR spectroscopy. PP, 2OA and LA conjugated PP were subsequently ligated with a recombinant peptide encoding aa177–252 of human PDC-E2 (PDC-228) using ILP to generate a 138 residue protein fragment corresponding to the residues 177–314 of PDC-E2.

Conjugation of lipoic acid and 2-octynoic acid to the 62 residue ILD peptide of PDC-E2 and ligation of PDC-228 with conjugated or unconjugated PP by IPL

NHS esters of LA and 2OA were prepared (4) and conjugated to the PP Lys259 and the protein concentrations of PP conjugated with 2OA (2OA-PP) and PP conjugated with LA (LA-PP) and thence quantified. Ligation of the PP peptide with the PDC-228 fragment was carried out by intein-mediated protein ligation to generate the PPL protein construct. The ligation for 2OA-PP and PDC-228 (2OA-PPL) was performed in a mixture consisting of 0.25 mg/ml PDC-228 0.4mg/ml 2OA-PP and 100 mM MESNA in the presence of 0.1 M Tris-HCl (pH 8.5) at 4°C for 5 days (Fig. 1).

Spin labeling and EPR spectroscopy analysis

We engineered the PDC-E2 ILD to contain two spin labels, since observation of either a change in spin-label dynamics or distance between the labels can serve as a reporter for the loop structure. As there was already a native cysteine at position 273 within this loop structure, position Ala253 was substituted with Cys to create a second site for targeting the MTSL spin label. The detection of distances via measuring the dipolar interaction of spin labels provides the ability to probe specific structural features of proteins in solution (15). Cys 253 and 273 of PP, 2OA-PP and LA-PP, PPL, LA-PPL and 2OA-PPL were spin labeled using the thio-specific nitroxide spin label [MTSL; (1-Oxyl-2,2,5,5-tetramethylpyrroline-3-methyl) methanethiosulfonate], a gift from Prof. Kalman Hideg, Pecs University. Unreacted spin label was removed by gel filtration chromatography. EPR measurements were conducted on a JEOL FA-100 EPR spectrometer using a TE_{011} cavity. Aliquots (25 μl) of purified peptide or ligated protein at described concentrations were loaded into a quartz flat cell and spectra were collected at room temperature (20–22°C) with 3 average scans each with 2-minutes of scan time and a 100 G sweep width at a microwave power of 3 mW. When included in the analyses, sample was incubated with Ficoll-70 (350 g/l final concentration) for 1 h. The rate of spin label rotational reorientation was calculated from the EPR line width and line height ratios (16) using: $\tau_c = 6.5 \times 10^{-10} (\Delta H_0) \left[\sqrt{\frac{I_0}{I_{+1}}} + \sqrt{\frac{I_0}{I_{-1}}} - 2 \right]$.

Identification of the immunoreactivity of PPL, LA-PPL and 2OA-PPL

To determine whether the 3 intein-mediated ligated proteins (PPL, LA-PPL and 2OA-PPL) still retained their AMA reactivity, they were analyzed by immunoblotting. A recombinant PDC-E2 peptide (rPDC-E2) containing the same backbone amino acid (177-314aa) (17) as the 3 ligated proteins was prepared and used as the positive control. Immunoreactivity was detected using horse-radish peroxidase conjugated anti-human immunoglobulin (IgG, IgM and IgA) as secondary (1:30,000 dilution) and chemiluminescence. ELISA plates were coated with either rPDC-E2, or LA-PPL, or 2OA-BSA and BSA (10μg/well in carbonate coating buffer) at 4°C overnight, blocked with 3% skim milk in PBC using our standard protocol with positive/negative controls (18).

An inhibition ELISA was set up to determine if a subpopulation of AMA specifically recognizes the molecular conformational change in 2OA-PPL peptide backbone induced by 2OA conjugation. A nested set of 30 sera including 15 PBC in stages I and II and 15 in stages III and stage IV that have been previously shown to react with both LA-PPL and 2OA-PPL, but not BSA were chosen. Individual samples were serially diluted and incubated with 1 ml of cyanogen bromide activated sepharose beads conjugated with 100ug of either 2OA-PPL, LA-PPL, 2OA-BSA, LA-PPL plus 2OA-BSA, BSA or human albumin (ALB) at 4°C overnight on a rocker. Absorbed sera were analyzed by ELISA to ensure complete absorption. The reactivity of the absorbed and unabsorbed sera against 2OA-PPL, LA-PPL and 2OA-BSA were determined by ELISA.

Preparation of affinity-purified antibodies

To further determine the specificities of the autoantibody population against 2OA-PPL, LA-PPL and 2OA, affinity-purified antibodies from 6 of the 13 PBC sera in group A, identified by inhibition ELISA, were prepared. Briefly, LA-PPL, 2OA-BSA or 2OA-PPL was separately conjugated to CNBr-activated sepharose beads. Individual selected serum samples were diluted 20 times with 10 mM Tris-HCl (pH 7.5) and filtered through 0.45 μm filter. The diluted serum was firstly passed through the CNBr-2OA-BSA column three times, washed and the bound anti-2OA antibodies were eluted off with 100 mM glycine (pH 2.5) and neutralized immediately with 1M Tris-HCl (pH 8.0). The flow-through was then passed through the CNBr-LA-PPL column and the anti-LA-PPL antibody was eluted under similar conditions. Thereafter, the flow-through fraction of CNBr-LA-PPL column was repassed through refreshed CNBr-LA-PPL and CNBr-2OA-BSA column 3–5 times to remove the antibodies against LA-PPL and 2OA-BSA till its reactivity against LA-PPL and 2OA-BSA could not be detected by ELISA. This final flow-through was then passed through the CNBr-2OA-PPL column and the remaining bound antibody was eluted with glycine elution buffer and neutralized using Tris-HCl, pH 8.0.

Epitope specificity and isotype determination of affinity purified antibodies

To determine the epitope specificity of the affinity purified antibody, in particular if there is an antibody population that recognizes only 2OA-PPL but not 2OA-BSA, PDC-E2, LA-PPL and PPL, the affinity purified fractions were analyzed by immunoblotting against 2OA-PPL, 2OA-BSA, PDC-E2, LA-PPL and PPL. Reactivity was determined using anti-human immunoglobulin (IgG, IgM and IgA) antibodies as secondary antibody (4). To further determine the Ig isotype of affinity purified antibodies, 96-well ELISA plates were coated with either 2OA-PPL, 2OA-BSA or LA-PPL and incubated with affinity purified fractions, antibodies against 2OA-BSA or LA-PPL, respectively.

Statistical analysis

Mean and standard deviation (SD) was used to describe and calculate the results from ELISA, inhibition ELISA. A two-tailed unpaired *t* test with Welch's correction was conducted to analyze the differences of antibodies reactivity against the modified proteins and the ratio of IgG/IgM. Enumeration data was analyzed by Fisher's exact test.

RESULTS

PPL, LA-PPL and 2OA-PPL ligation products are reactive with AMA

The inner lipoyl domain (ILD) of PDC-E2 encompasses residues spanning positions 250 to 314. To generate a PDC protein construct that would facilitate modifications of Lys259, we used intein-mediated ligation to join the 76 residue PDC-228 peptide with the 62 residue ILD peptide (PP, LA-PP or 2OA-PP) to generate PPL and 2OA-PPL (Fig. 2A). We tested the resulting ligation products for recognition by immunoblotting with AMA positive sera. As shown in Figure 2B, AMA readily react with PPL, LA-PPL and 2OA-PPL, providing reagents that appear as immunological mimics of PDC-E2. Next, we analyzed the specificity of serum samples from patients with PBC, PSC and HC against LA-PPL and for purposes of peptide control 2OA-BSA by ELISA. We also screened aliquots of the same sera against rPDC-E2 and BSA that served as positive and negative controls. As expected, PBC sera reacted to rPDC-E2, LA-PPL and 2OA-BSA but not BSA. None of the sera from PSC and HC reacted to either rPDC-E2, LA-PPL, 2OA-BSA or BSA (Fig. 3). In the HC group, the mean reactivity (O.D. +/− 2 S.D.) of the sera against rPDC-E2, LA-PPL and 2OA-BSA were 0.1635, 0.1609, and 0.0877, respectively. Using these OD readings as the positive or negative cutoff values of autoantibody to the corresponding proteins, sera from PBC demonstrate rates of reactivity against rPDC-E2, LA-PPL and 2OA-BSA of 92.19% (118/128), 94.53% (121/128) and 46.88% (61/128), respectively.

Immunoabsorption analysis identified an AMA subpopulation specific to 2OA-PPL

To determine if there is a subpopulation of antibodies with specificity for 2OA-PPL, but not for LA-PPL and 2OA in PBC patients, sera from 30 PBC patients which have been previously determined to recognize both LA-PPL and 2OA-BSA were absorbed with either 2OA-PPL, LA-PPL, or 2OA-BSA individually and also a mixture containing both LA-PPL and 2OA-BSA. As negative controls, serum samples were also absorbed with BSA and human albumin. The absorbed serum samples were analyzed for their reactivity to 2OA-PPL, LA-PPL and 2OA-BSA at 1:250, 1:500, 1:1,000 and 1: 2,000 sera dilution (Fig. 4) by ELISA.

All serum samples absorbed with 2OA-PPL lost almost all of their reactivity to 2OA-PPL. Serum samples absorbed with either human albumin or BSA or 2OA-BSA retained almost 100% of their reactivity to 2OA-PPL (Fig. 4A and B). The pattern of reactivity of sera following absorption with a mixture of LA-PPL + 2OA-BSA led us to divide the sera into 2 groups, Group A sera being those sera that following absorption with LA-PPL + 2-OA-BSA still reacted with 2AO-PPL and Group B that failed to show residual activity against 2AO-PPL. As seen in Fig. 6A and B, 13/30 serum samples were classified as belonging to Group A and the remaining 17/30 to Group B. We interpret these findings as evidence for the presence of antibodies not only to LA-PPL and 2-OA but that a significant fraction of PBC sera (43.3%) in addition contain antibodies with specificity for 2OA-PPL.

When absorbed sera were assayed for their reactivity to LA-PPL (Fig. 4C and D), all sera absorbed with LA-PPL lost nearly all of their reactivity to LA-PPL. Serum samples absorbed with either human albumin or BSA or 2OA-BSA retained almost 100% of their

reactivity to 2LA-PPL. Sera absorbed with a combination of 2OA-BSA and LA-PPL lost all their reactivity to LA-PPL. Interestingly, sera absorbed with 2OA-PPL lost most but not all of their reactivity to LA-PPL, suggesting there is another subpopulation of antibodies that only recognize LA-PPL. When absorbed sera were assayed for their reactivity to 2OA-BSA (Fig. 4E and F), samples absorbed with either human albumin or BSA retained almost 100% of their reactivity to 2OA-BSA. Sera samples absorbed with LA-PPL also retained almost 100% reactivity to 2OA-BSA indicating the presence of 2OA specific antibodies in PBC. Sera samples absorbed with 2OA-BSA, 2OA-PPL and a mixture of 2OA-BSA plus LA-PPL lost almost all of their reactivity to 2OA-BSA.

Affinity purified antibody to the 2OA-PPL altered PDC-E2 backbone do not recognize 2OA-BSA and LA-PPL and are predominantly IgM

We have identified a unique subpopulation of AMA that specifically recognize the altered molecular structural on the backbone of 2OA-PPL caused by 2OA conjugation. Immunoblotting showed that the purified sub-population of antibodies against 2OA-PPL, only recognized 2OA-PPL, but not LA-PPL, 2OA-BSA, PPL or rPDC-E2 (Fig. 5A). More importantly IgG/IgM ratio among the antibodies against LA-PPL, 2OA-BSA and 2OA-PPL were significantly different. The predominant antibody to LA-PPL was composed of IgG. In contrast, the antibody with specificity for 2OA-PPL and the antibody against 2OA-BSA were mainly IgM (Fig. 5B, C).

AMA subpopulation specific to 2OA-PPL structure induced by 2OA conjugation are present predominantly in early stages of PBC

Next, we compared the reactivity of sera from the 13 patients with antibody with specificity for 2OA-PPL in Group A and sera from the remaining 17 patients in Group B with respect to their age, gender ratio and stage of disease. There are no significant differences between the two groups in age and gender ratio between the two groups. However, a high frequency (10/13) of patients within Group A belonged to patients with early stage PBC disease (66.67%) and a minor subset (3/13) belonged to patients in late stage (P= 0.025) (Supplemental Table 2).

EPR analysis indicated a marked structural change in 2OA-PPL

We set out to determine whether conjugation of 2OA to the inner lipoyl domain may result in unsuspected structural alterations and creation of a neo-epitope. There is a fair degree of chemical similarity between 2-OA and lipoic acid so this would be somewhat surprising. The lysine at position 259 is the residue at which lipoyl addition occurs in native PDC-E2 ILD. Molecular structure analysis of this lipoylated molecule shows that it folds as a loop (19). To determine how the structure of this region relates to antigenicity, we analyzed the dynamics of PPL, LA-PPL and 2OA-PPL using EPR spectroscopy of spin labels attached simultaneously at positions 253 and 273. Both positions reacted with the thio-specific nitroxide spin label MTSL and additionally we made a construct with alanine substituted for cysteine at position 253.

The EPR spectra of the spin-labeled PP, with and without ligation to PDC-228 are shown in Figure 6. Samples were measured at 1 mg/ml protein as determined by BCA protein assay

and were plotted as normalized to the same molar concentration of each polypeptide. Because of the relatively small size of both the free and ligated ILD peptides (6.8 and 14.7 kD, respectively), a fast rate of global tumbling in solution is expected to significantly contribute to the motional averaging of the EPR spectra. Thus samples were examined under high viscosity (30% ficoll) to decrease the rate of global tumbling. The EPR spectra of the ILD peptides in ficoll contain narrow lines and are largely isotropic, indicating a high degree of dynamic disorder. An empirical estimation of the rates of motion is given in Supplemental Table 1.

As shown in Figure 6A, the sharp EPR spectrum of the ILD peptide (PP) reflects a high level of motional freedom arising from both spin labels. Following ligation with the PDC-228 peptide, the intensity of EPR spectrum decreases significantly. However, the spectral line shape does not display features of a strongly immobilized label, indicating the spin labels remain in a relatively dynamic environment following ligation. Given the lack of spectral change, the broadening can largely be attributed to the rapid modulation of the dipolar interaction between labels (20). Magnetic interaction between spins becomes strong enough to affect the spectrum when the nitroxides are within 2 nm of each other (21). Thus PDC228 facilitates the formation of the ILD loop conformation, placing positions 253 and 273 within a close proximity of one another.

When the PP and PPL were ligated with LA and 2OA the results obtained show dramatically different outcomes with respect to a dipolar interaction between the spin labels attached at positions 253 and 273. Thus, while the sample with lipoic acid displays a level of spectral broadening similar to the unmodified protein (Fig. 6B), lipoylation with 2OA does not result in a broadened EPR spectrum (Fig. 6C). This indicates the loop structure of the lipoyl domain remains intact with lipoic acid modification, but upon modification with 2OA, became incapable of positioning the spins within a close (<2 nm) proximity. A comparison of the ligated samples with and without lipoylation is shown in Figure 7. The correlation time of the faster motion within the ensemble can be estimated from the empirical relation given in Eqn 1 (Methods). The estimated correlation times of the spectra in Figures 6A–C are given in Supplemental Table 1. Following ligation, the estimated rate of motion of the labels in lipoylated samples are approximately 50% faster, suggesting that while ligation with lipoic acid has some dynamic effects on the ILD loop, the effects are not substantial enough to disrupt its hairpin structure.

Affinity purified AMA alters the EPR spectrum of 2OA-PPL but not LA-PPL

Because EPR analysis of spin labels within the ILD loop can distinguish conformational states induced by either lipoic acid or 2OA, we then measured the response of each sample to the presence of AMA. The effect of AMA on the EPR spectra of spin-labeled ILD protein is shown in Figure 8. While the addition of an aliquot of antibody with specificity for 2OA-PPL (1mg/ml final concentration) from AMA-positive sera to 1 mg/ml of the protein construct did not affect the EPR spectrum of LA-PPL, the addition of an aliquot of the same antibody to 2OA-PPL results in the appearance of a spin exchange-broadened component to the EPR spectrum (Fig. 8b).

DISCUSSION

Accumulating evidence implicates both genetic susceptibility (22–27) and environmental insults (28–30) that contribute to the etiology of PBC. However the underlying mechanism leading to loss of self-tolerance remains an enigma. This is an issue throughout autoimmunity, often called searching for the Holy Grail (2, 31–36). Using high-resolution structural analysis and modeling studies on the lipoyl domains of PDC-E2, LA is prominently displayed on the outer surface of PDC-E2 and rotates by means of a “swinging arm” with respect to the bulk of the molecule (19). In PDC-E2, LA is covalently attached with the ε group of lysine (Lys259) by an amide bond. LA contains two sulfur atoms at C6 and C8, which are connected by a disulfide bond. During this biochemical process, the LA dithionate ring is susceptible to xenobiotic modifications, particularly in the biliary tract. Lipoate-protein ligase catalyzes the covalent attachment of LA to Lys259 on the PDC-E2 lipoyl domain in a two-step reaction, during which a variety of other carboxylic acids including those without the dithiolane ring (such as some xenobiotic chemicals) could also be transferred to Lys259 (37, 38). In previous studies, we demonstrated that when PDC-E2 Lys259 was chemically conjugated with chemicals with similar molecular structures to LA, immune self-tolerance to PDC-E2 could be broken via cross reactive immune responses against the LA. Such similar chemicals included 2OA (5). However the structural effect of xenobiotic conjugation at Lys259 on the PDC- PP peptide backbone, and the immunological consequences of such conformational alterations were unknown (8, 39, 40). 2-OA methyl esters are widely used in cosmetics, lipstick, chewing gums and foods additives (41).

Our intein-mediated ligation approach not only facilitates the targeting of the 2OA and LA conjugations at Lys259, but provides a method to label the protein construct via site-directed labeling of Cys in the PP peptide. We engineered the PP to contain an additional Cys residue, by substituting Ala253 with Cys. Thus the ligated PP peptides contained 2 Cys residues for labeling (position 253 and the native Cys273). These thiols allow for specific attachment of the MTS spin labels and subsequent EPR analysis to probe the structural consequences of conjugation with LA and the xenobiotic 2OA. Two spin labels within the inner lipoyl domain is advantageous since the observation of either a change in spin-label dynamics or distance between the labels can serve as a reporter for the loop structure. To our knowledge this is the first application of intein-mediated protein ligation for targeting of lipoylation and the incorporation of spin labels into a protein.

It is important to demonstrate that PPL, LA-PPL and 2OA-PPL are each immune-reactive to AMA and this was shown by immunoblotting (Fig. 2). This is of significance because they were all ligated by intein chemistry, residue Ala253 of PDC-E2 was substituted by cysteine and Lys259 was also chemically distinct from one another, with or without hapten conjugation (Fig. 2B). Thus, AMA reactivity to PDC-E2 was directed to the inner lipoyl domain of PDC-E2, which could be in either native or modified form. EPR analysis of the spin-labeled peptide constructs was then carried out to probe the structural consequences of lipoylation with LA and the xenobiotic mimic 2-OA. The continuous wave approach applied in this study allows for the detection of spin pairs within 2 nm of each other. The results by EPR indicate positions 253 and 273 in the ILD loop are on the order of 1–1.5 nm from each other, given the magnitude of broadening and the absence of spectral distortion due to spin

exchange. The absence of broadening in protein lipoylated with 2OA demonstrates positions 253 and 273 become separated by at least 2 nm, although these positions could in theory become separated by as much as 7 nm if the region were to fully extend.

From EPR, we noticed that there is a clear conformational difference between the 2OA-PPL and LA-PPL protein constructs. To investigate if this change on 2OA-PPL could induce a specific subpopulation in AMA in PBC, or in other words, if this change induced any specific immune response in PBC, an inhibition ELISA was conducted (Fig. 4). The differences in inhibition ELISA imply the presence of an antibody subpopulation, which specifically recognized the epitopes on the backbone of PDC-E2 induce by 2OA modification. Furthermore, in both groups, sera absorbed by 2OA-BSA showed no obvious influence for its reactivity to 2OA-PPL, just as the sera absorbed by negative control BSA and ALB did (Fig. 4A, B). Thus, it can be inferred that the antibody to the hapten 2OA plays a minor role in the reactivity of the sera against the backbone of PDC-E2. Similarly, the reactivity to 2OA and LA is also reflected in difference in reactivity to LA-PPL between the sera absorbed by 2OA-PPL and LA-PPL between groups A and B (Fig. 4C, D). In both Groups A and Group B, serum reactivity to 2OA-BSA was not influenced by LA-PPL adsorption (Fig. 4E, F).

Based on inhibition ELISA data, affinity purified antibody with specificity for 2OA-PPL, antibodies with specificity for LA-PPL and antibody to hapten 2OA were separately obtained from six serum samples from Group A. The antibodies against 2OA-PPL were further studied by immunoblotting in which this purified antibody could only recognize 2OA-PPL, but not 2OA-BSA, rPDC-E2, LA-PDC and PPL (Fig. 5A). Interestingly, the isotype of the three antibodies (antibody to 2OA-PPL, antibody to LA-PPL and antibody to 2OA) were significantly different though they were purified from the same PBC patients (Fig. 5B, C). The antibody to 2OA was predominantly IgM isotype, which was similar with the isotype of antibody to 6,8-bis(acetylthio) octanoic acid (SAc), one of the other xenobiotic lipoyl mimic (4). The isotype of antibody to LA-PPL was predominantly IgG, as expected. More interestingly, the IgG/IgM ratio of the affinity antibody against 2OA-PPL was between that of antibody against LA-PPL and of antibody against 2OA (Fig. 5B, C). It is reasonable that 2OA itself might trigger an immunological response to produce antibody against 2OA when 2OA is conjugated on Lys259 of PDC-E2 at the early induction phase. As the response progresses, autoantibody to the backbone of PDC-E2 are produced through epitope spreading from 2OA to the PDC-E2 backbone. By the usual processes of somatic mutation and antibody affinity maturation, the isotype of autoantibody to the peptide backbone of PDC-E2 will switch from IgM to predominantly IgG (42). We suggest that the coupling of a xenobiotic induces a conformational change that renders the ILD of PDC-E2 distinctly structurally altered to an extent where it is recognized as foreign but with enough preserved structure such that induced antibodies cross-react to authentic LA conjugated PDC-E2. This occurs early in the process of tolerance breakdown explaining why anti 2OA-ILD antibodies are enriched for IgM in early stage disease. The natural history of PBC clearly begins with a break of tolerance and the data herein emphasizes these events. As the disease evolves, there will be additional effector pathways activated which will include both innate and adaptive immunity. The relative roles of each of these pathways to both the initial loss of tolerance and then the subsequent continued adaptive response reflects what we have

previously called a multi-orchestrated immune response and may likely be different during the evolution of disease (43)

Supplementary Material

Refer to Web version on PubMed Central for supplementary material.

Acknowledgments

Funding: This work is supported in part by NIH grants DK067003 and DK39588.

List of Abbreviations

2OA	2-octynoic acid
2OA-BSA	BSA conjugated with 2OA
2OA-PP	PP conjugated with 2OA
2OA-PPL	ligation product of PDC-228 and PP conjugated with 2OA
ALB	human albumin
AMA	antimitochondrial antibodies
BSA	bovine serum albumin
ELISA	enzyme linked immunosorbent assay
EPR	electron paramagnetic resonance
HC	healthy controls
ILD	Inner Lipoyl domain
IPL	intein-mediated protein ligation
LA	lipoic acid
LA-PP	PP conjugated with LA
LA-PPL	ligation product of PDC-228 and PP conjugated with LA
MTS	methanethiosulfonate (1-Oxyl-2,2,5,5-tetramethylpyrroline-3-methyl)
PBC	primary biliary cholangitis
PCR	Polymerase chain reaction
PDC-228	recombinant peptide corresponding to aa177–252 of human PDC-E2
PDC-E2	E2 subunit of pyruvate dehydrogenase
PP	synthetic peptide corresponding to aa253–314 of PDC-E2

PPL	PDC-228 and PP ligation
PSC	primary sclerosing cholangitis
rPDC-E2	recombinant PDC-E2

References

1. Bowlus CL, Gershwin ME. The diagnosis of primary biliary cirrhosis. Autoimmun Rev. 2014; 13:441–444. [PubMed: 24424173]
2. Leung PS, Choi J, Yang G, Woo E, Kenny TP, Gershwin ME. A contemporary perspective on the molecular characteristics of mitochondrial autoantigens and diagnosis in primary biliary cholangitis. Expert Rev Mol Diagn. 2016; 16:697–705. [PubMed: 26953925]
3. Tana MM, Shums Z, Milo J, Norman GL, Leung PS, Gershwin ME, Noureddin M, et al. The Significance of Autoantibody Changes Over Time in Primary Biliary Cirrhosis. Am J Clin Pathol. 2015; 144:601–606. [PubMed: 26386081]
4. Chen RC, Naiyanetr P, Shu SA, Wang J, Yang GX, Kenny TP, Guggenheim KC, et al. Antimitochondrial antibody heterogeneity and the xenobiotic etiology of primary biliary cirrhosis. Hepatology. 2013; 57:1498–1508. [PubMed: 23184636]
5. Amano K, Leung PS, Rieger R, Quan C, Wang X, Marik J, Suen YF, et al. Chemical xenobiotics and mitochondrial autoantigens in primary biliary cirrhosis: identification of antibodies against a common environmental, cosmetic, and food additive, 2-octynoic acid. J Immunol. 2005; 174:5874–5883. [PubMed: 15845458]
6. Naiyanetr P, Butler JD, Meng L, Pfeiff J, Kenny TP, Guggenheim KG, Reiger R, et al. Electrophile-modified lipoic derivatives of PDC-E2 elicits anti-mitochondrial antibody reactivity. J Autoimmun. 2011; 37:209–216. [PubMed: 21763105]
7. Rieger R, Leung PS, Jeddeloh MR, Kurth MJ, Nantz MH, Lam KS, Barsky D, et al. Identification of 2-nonynoic acid, a cosmetic component, as a potential trigger of primary biliary cirrhosis. J Autoimmun. 2006; 27:7–16. [PubMed: 16876981]
8. Wakabayashi K, Lian ZX, Leung PS, Moritoki Y, Tsuneyama K, Kurth MJ, Lam KS, et al. Loss of tolerance in C57BL/6 mice to the autoantigen E2 subunit of pyruvate dehydrogenase by a xenobiotic with ensuing biliary ductular disease. Hepatology. 2008; 48:531–540. [PubMed: 18563844]
9. Wang J, Yang GX, Tsuneyama K, Gershwin ME, Ridgway WM, Leung PS. Animal models of primary biliary cirrhosis. Semin Liver Dis. 2014; 34:285–296. [PubMed: 25057952]
10. Wang J, Budamagunta MS, Voss JC, Kurth MJ, Lam KS, Lu L, Kenny TP, et al. Antimitochondrial antibody recognition and structural integrity of the inner lipoyl domain of the E2 subunit of pyruvate dehydrogenase complex. J Immunol. 2013; 191:2126–2133. [PubMed: 23894195]
11. Bambha K, Kim WR, Talwalkar J, Torgerson H, Benson JT, Therneau TM, Loftus EV Jr, et al. Incidence, clinical spectrum, and outcomes of primary sclerosing cholangitis in a United States community. Gastroenterology. 2003; 125:1364–1369. [PubMed: 14598252]
12. Beuers U, Gershwin ME, Gish RG, Invernizzi P, Jones DE, Lindor K, Ma X, et al. Changing nomenclature for PBC: from ‘cirrhosis’ to ‘cholangitis’. Gastroenterology. 2015; 149:1627–1629. [PubMed: 26385706]
13. Leung PS, Rossaro L, Davis PA, Park O, Tanaka A, Kikuchi K, Miyakawa H, et al. Antimitochondrial antibodies in acute liver failure: implications for primary biliary cirrhosis. Hepatology. 2007; 46:1436–1442. [PubMed: 17657817]
14. Stravitz RT, Lefkowitch JH, Fontana RJ, Gershwin ME, Leung PS, Sterling RK, Manns MP, et al. Autoimmune acute liver failure: proposed clinical and histological criteria. Hepatology. 2011; 53:517–526. [PubMed: 21274872]
15. Eaton, SS., Eaton, GR. Measurements of Interspin Distances by EPR Electron Paramagnetic Resonance. In: Gilbert, M.Davies, M., Murphy, D., editors. Electron Paramagnetic Resonance. Royal Society of Chemistry; London: 2004. p. 318-337.

16. Cannon B, Polnaszek CF, Butler KW, Eriksson LE, Smith IC. The fluidity and organization of mitochondrial membrane lipids of the brown adipose tissue of cold-adapted rats and hamsters as determined by nitroxide spin probes. Arch Biochem Biophys. 1975; 167:505–518. [PubMed: 164831]
17. Moteki S, Leung PS, Coppel RL, Dickson ER, Kaplan MM, Munoz S, Gershwin ME. Use of a designer triple expression hybrid clone for three different lipoyl domain for the detection of antimitochondrial autoantibodies. Hepatology. 1996; 24:97–103. [PubMed: 8707289]
18. Liu H, Norman GL, Shums Z, Worman HJ, Krawitt EL, Bizzaro N, Vergani D, et al. PBC screen: an IgG/IgA dual isotype ELISA detecting multiple mitochondrial and nuclear autoantibodies specific for primary biliary cirrhosis. J Autoimmun. 2010; 35:436–442. [PubMed: 20932720]
19. Howard MJ, Fuller C, Broadhurst RW, Perham RN, Tang JG, Quinn J, Diamond AG, et al. Three-dimensional structure of the major autoantigen in primary biliary cirrhosis. Gastroenterology. 1998; 115:139–146. [PubMed: 9649469]
20. McHaourab HS, Oh KJ, Fang CJ, Hubbell WL. Conformation of T4 lysozyme in solution. Hinge-bending motion and the substrate-induced conformational transition studied by site-directed spin labeling. Biochemistry. 1997; 36:307–316. [PubMed: 9003182]
21. Altenbach C, Oh KJ, Trabanino RJ, Hideg K, Hubbell WL. Estimation of inter-residue distances in spin labeled proteins at physiological temperatures: experimental strategies and practical limitations. Biochemistry. 2001; 40:15471–15482. [PubMed: 11747422]
22. Cordell HJ, Han Y, Mells GF, Li Y, Hirschfield GM, Greene CS, Xie G, et al. International genome-wide meta-analysis identifies new primary biliary cirrhosis risk loci and targetable pathogenic pathways. Nat Commun. 2015; 6:8019. [PubMed: 26394269]
23. Hirschfield GM, Liu X, Han Y, Gorlov IP, Lu Y, Xu C, Lu Y, et al. Variants at IRF5-TNPO3, 17q12–21 and MMEL1 are associated with primary biliary cirrhosis. Nat Genet. 2010; 42:655–657. [PubMed: 20639879]
24. Liu X, Invernizzi P, Lu Y, Kosoy R, Lu Y, Bianchi I, Podda M, et al. Genome-wide meta-analyses identify three loci associated with primary biliary cirrhosis. Nat Genet. 2010; 42:658–660. [PubMed: 20639880]
25. Mells GF, Floyd JA, Morley KI, Cordell HJ, Franklin CS, Shin SY, Heneghan MA, et al. Genome-wide association study identifies 12 new susceptibility loci for primary biliary cirrhosis. Nat Genet. 2011; 43:329–332. [PubMed: 21399635]
26. Webb GJ, Siminovitch KA, Hirschfield GM. The immunogenetics of primary biliary cirrhosis: A comprehensive review. J Autoimmun. 2015; 64:42–52. [PubMed: 26250073]
27. Webb GJ, Hirschfield GM. Using GWAS to identify genetic predisposition in hepatic autoimmunity. J Autoimmun. 2016; 66:25–39. [PubMed: 26347073]
28. Ala A, Stanca CM, Bu-Ghanim M, Ahmado I, Branch AD, Schiano TD, Odin JA, et al. Increased prevalence of primary biliary cirrhosis near Superfund toxic waste sites. Hepatology. 2006; 43:525–531. [PubMed: 16496326]
29. Leung PS, Wang J, Naiyanetr P, Kenny TP, Lam KS, Kurth MJ, Gershwin ME. Environment and primary biliary cirrhosis: electrophilic drugs and the induction of AMA. J Autoimmun. 2013; 41:79–86. [PubMed: 23352659]
30. Selmi C, Balkwill DL, Invernizzi P, Ansari AA, Coppel RL, Podda M, Leung PS, et al. Patients with primary biliary cirrhosis react against a ubiquitous xenobiotic-metabolizing bacterium. Hepatology. 2003; 38:1250–1257. [PubMed: 14578864]
31. Floreani A, Leung PS, Gershwin ME. Environmental Basis of Autoimmunity. Clin Rev Allergy Immunol. 2016; 50:287–300. [PubMed: 25998909]
32. Hisamoto S, Shimoda S, Harada K, Iwasaka S, Onohara S, Chong Y, Nakamura M, et al. Hydrophobic bile acids suppress expression of AE2 in biliary epithelial cells and induce bile duct inflammation in primary biliary cholangitis. J Autoimmun. 2016
33. Lleo A, Bowlus CL, Yang GX, Invernizzi P, Podda M, Van de Water J, Ansari AA, et al. Biliary apotopes and anti-mitochondrial antibodies activate innate immune responses in primary biliary cirrhosis. Hepatology. 2010; 52:987–998. [PubMed: 20568301]
34. Mattalia A, Luttig B, Rosina F, Leung PS, Van de Water J, Bauducci M, Ciancio A, et al. Persistence of autoantibodies against recombinant mitochondrial and nuclear pore proteins after

orthotopic liver transplantation for primary biliary cirrhosis. J Autoimmun. 1997; 10:491–497. [PubMed: 9376077]

35. Mayo MJ. Natural history of primary biliary cirrhosis. Clin Liver Dis. 2008; 12:277–288. viii. [PubMed: 18456180]
36. Rong G, Zhong R, Lleo A, Leung PS, Bowlus CL, Yang GX, Yang CY, et al. Epithelial cell specificity and apotope recognition by serum autoantibodies in primary biliary cirrhosis. Hepatology. 2011; 54:196–203. [PubMed: 21488079]
37. Brookfield DE, Green J, Ali ST, Machado RS, Guest JR. Evidence for two protein-lipoylation activities in Escherichia coli. FEBS Lett. 1991; 295:13–16. [PubMed: 1765143]
38. Reed KE, Morris TW, Cronan JE Jr. Mutants of Escherichia coli K-12 that are resistant to a selenium analog of lipoic acid identify unknown genes in lipoate metabolism. Proc Natl Acad Sci U S A. 1994; 91:3720–3724. [PubMed: 8170976]
39. Katsumi T, Tomita K, Leung PS, Yang GX, Gershwin ME, Ueno Y. Animal models of primary biliary cirrhosis. Clin Rev Allergy Immunol. 2015; 48:142–153. [PubMed: 25771770]
40. Hsueh YH, Chang YN, Loh CE, Gershwin ME, Chuang YH. AAV-IL-22 modifies liver chemokine activity and ameliorates portal inflammation in murine autoimmune cholangitis. J Autoimmun. 2016; 66:89–97. [PubMed: 26537567]
41. Arctander, S. Methyl heptine carbonate. In: Arctander, S., editor. Perfume and Flavor Chemicals (Aroma Chemicals). Vol. 2. Wheaton, IL: Allured Publishing; 1994. p. 2045
42. Jung S, Schickel JN, Kern A, Knapp AM, Eftekhari P, Da Silva S, Jaulhac B, et al. Chronic bacterial infection activates autoreactive B cells and induces isotype switching and autoantigen-driven mutations. Eur J Immunol. 2016; 46:131–146. [PubMed: 26474536]
43. Gershwin ME, Ansari AA, Mackay IR, Nakanuma Y, Nishio A, Rowley MJ, Coppel RL. Primary biliary cirrhosis: an orchestrated immune response against epithelial cells. Immunol Rev. 2000; 174:210–225. [PubMed: 10807518]

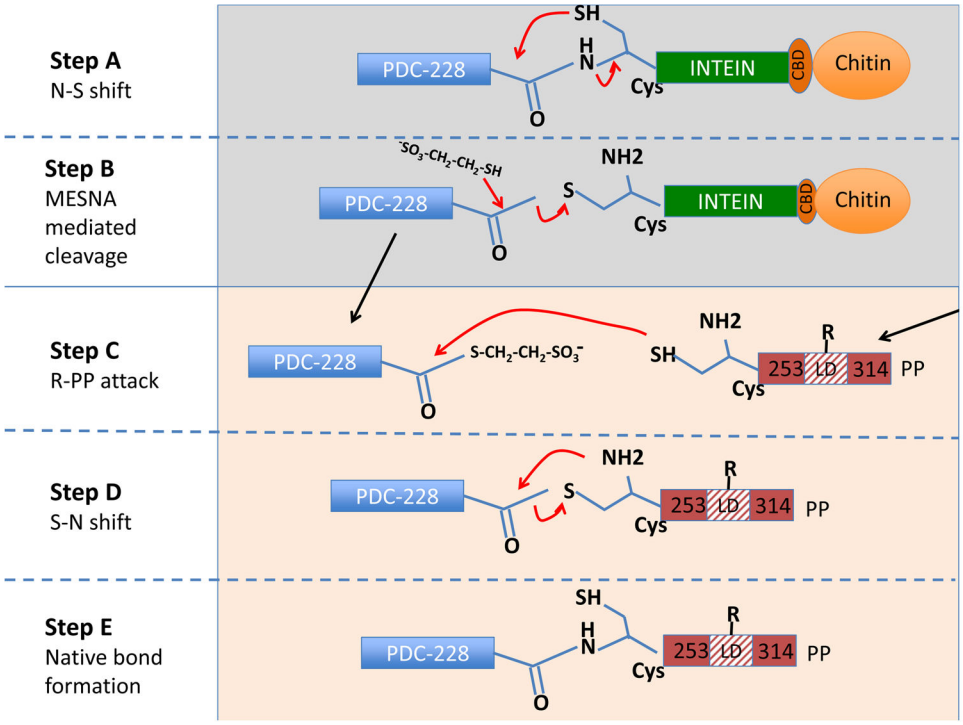

Figure 1.

Schematic diagram of intein-mediated protein ligation (IPL) between PDC-228 and conjugated PP. Lysates of E. coli expressing PDC-228 recombinant protein is mixed with chitin resin. PDC-228 is attached via the intein-chitin binding domain (CBD) by peptide linkage between leucine (Leu) residue on the C- terminus of PDC-228 and cysteine (Cys) residue on the N- terminus of intein with the chitin resin for affinity purification of PDC-228. 2-mercaptoethanesulfonic acid (MESNA) is used as the thiol reagent to induce intein-mediated cleavage on column when the chemical bond between the Leu and Cys residue undergoes a spontaneous N-S acyl shift, which produces a C-terminal thioester of PDC-228 (Step A and Step B). Thereafter, the C-terminus of PDC-228 is attacked by the Cys on the N-terminal of PP or xenobiotic modified PP and can then be covalently ligated with each other (Step C and D). Finally, a native peptide bond between the PDC-228 and PP or xenobiotic modified PP is generated by the spontaneous S-N acyl shift, and the ligated product 2OA-PPL is obtained (Step E). PDC-228: recombinant peptide spans aa177-252 of the human PDC-E2; PP, synthetic peptide spans aa253–314 of PDC-E2; LD: lipoyl domain; R: 2OA or LA.

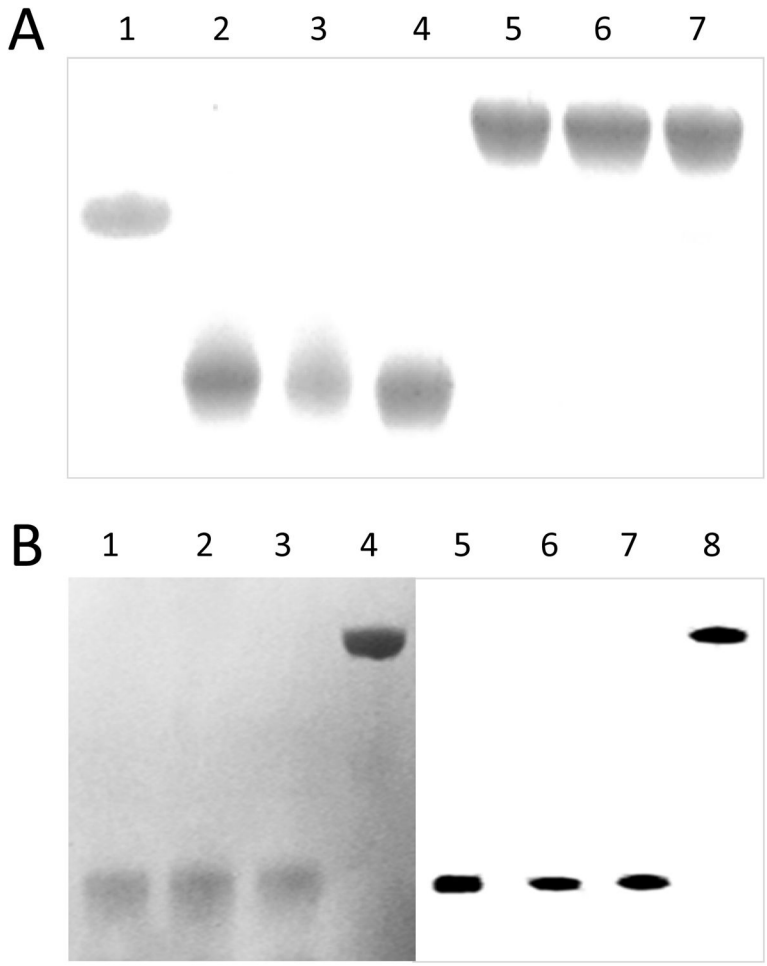

Figure 2.

Gel electrophoresis and immunoblot analysis of PDC-228 and intein constructs. 2A. SDS-PAGE analysis of PDC-228 (lane 1), PP (lane 2), LA-PP (lane 3; 2OA-PP (lane 4); PPL (lane 5); LA-PPL (lane 6) and 2OA-PPL (lane 7). 2B. SDS-PAGE (lanes 1–4) and (lanes 5–8) Immunoblot analysis of PPL (lane 1, 5); LA-PPL (lane 2, 6); 2OA-PPL (lane 3,7) and rPEC-E2 (lane 4, 8). Note that all the three ligations and rPDC-E2 reacted with AMA (+) serum. Serum samples from AMA negative PBC patients and HC do not react.

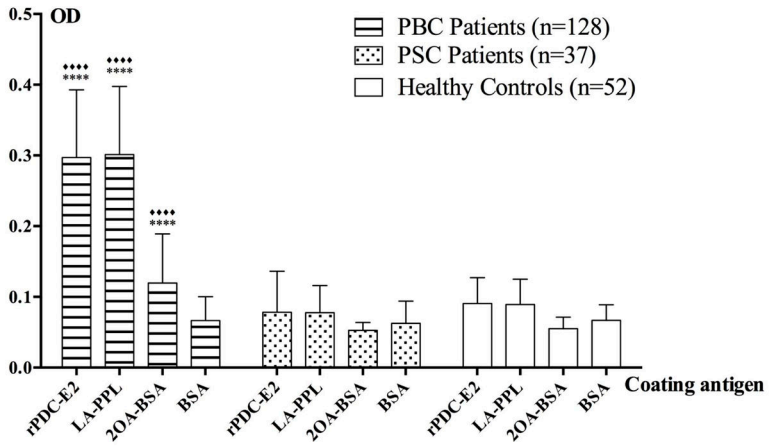

Figure 3.

Ig reactivity of serum samples from patient with PBC (n=128) against rPDC-E2, LA-PPL, 2OA-BSA and BSA by ELISA. Patients with PSC (n=37) and HC (n=52) were studied in parallel. Note that the reactivity of antibody against rPDC-E2, LA-PPL and 2OA-BSA detected only in PBC but not in PSC patients and HC. Data presented as mean±SD. Asterisks (****) and rhombus (◆◆◆◆;) indicate significant differences (P<0.0001, two-tailed unpaired t test with Welch's correction).

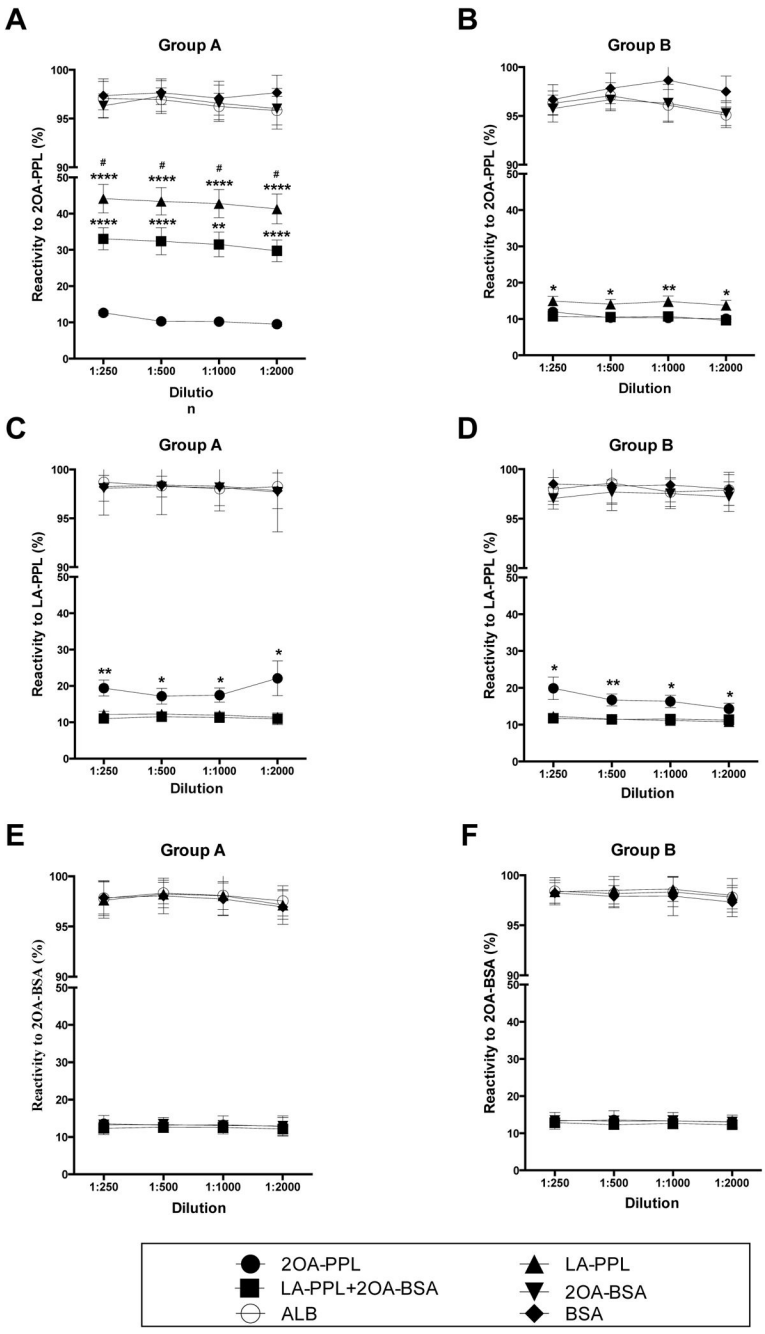

Figure 4.

Inhibition ELISA of PBC serum against 2OA-PPL, LA-PPL and 2OA-BSA. Serum from 30 AMA positive PBC sera were individually absorbed with 2OA-PPL, LA-PPL, 2OA-BSA and dually absorbed with combination of LA-PPL and 2OA-BSA. Serum samples absorbed separately by BSA and ALB were included as controls. Based on the reactivity pattern of the absorbed serum samples to 2OA-PPL, we noted that the 30 selected PBC samples with both antibodies to LA-PPL and 2OA-BSA could be divided into either Group A and Group B. In Group A (n=13), serum samples absorbed with the combination of LA-PPL and 2OA-BSA

could retain a significant higher reactivity to 2OA-PPL while in Group B (n=17), serum samples absorbed by with the combination of LA-PPL and 2OA-BSA did not show any difference in of their reactivity to 2OA-PPL. This data suggested the possible presence of a subpopulation of AMA with specificity to 2OA-PPL but not LA-PPL and 2OA existed in the Group A serum samples (Fig A and B). The serum samples absorbed by LA-PPL in Group A had distinctively higher reactivity than those absorbed by the combined adsorption whereas this difference in reactivity to 2OA-PPL was not significant in Group B, which indirectly supported the existence of an AMA subpopulation that recognize 2OA-PPL but not LA-PPL and 2OA (A, B). The serum samples absorbed with 2OA-PPL in both group remained reactive to LA-PPL (C, D). However, when they were absorbed by any proteins containing 2OA-PPL, their reactivity to 2OA-BSA were similar to serum samples absorbed by 2OA-BSA (E, F). Moreover, serum reactivity to 2OA-BSA was not affected by LA-PPL absorption in both groups (Fig. 5E, F). Data presented as mean ± SEM. The two-tailed unpaired *t* test with Welch's correction was employed to analyze all the differences between absorbed serum reactivity. * indicated statistically significant difference compared with 2OA-PPL absorption (*P<0.05, **P<0.01, ****P<0.001). # indicated statistically significant difference compared with the combined absorption of LA-PPL and 2OA-BSA (#P<0.05). ※ indicated statistically significant difference compared with the LA-PPL absorption (※P<0.05, ※※P<0.01).

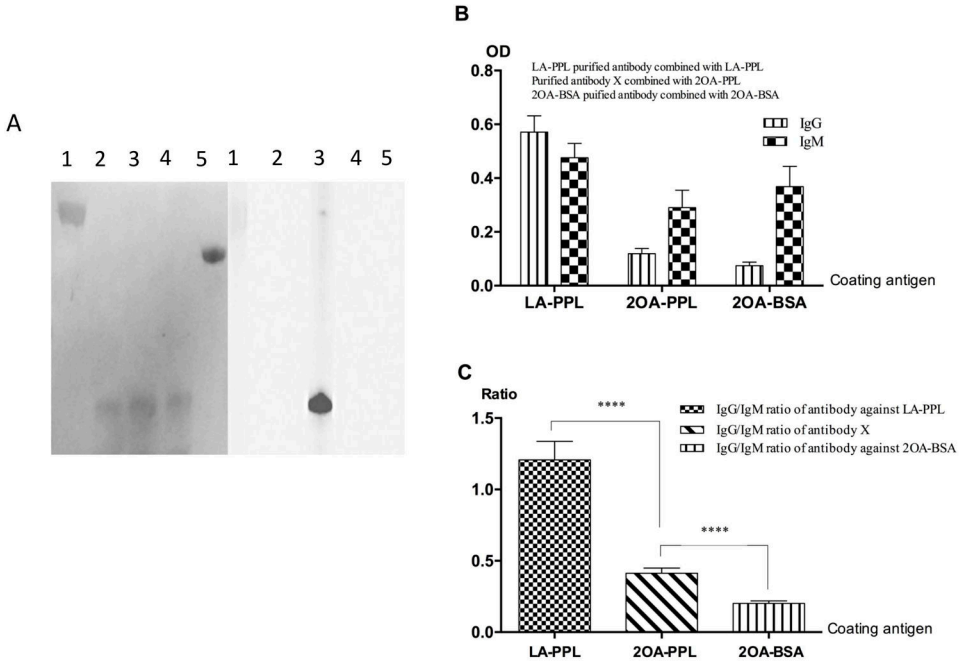

Figure 5.

Epitope specificity of affinity purified antibodies and Ig isotype analysis. Affinity purified antibodies were prepared by multi-step affinity purification process as described in the Methods section and analyzed for their reactivity against 2OA-BSA (lane1), PPL (lane 2), 2OA-PPL (lane 3), LA-PPL (lane 4) and rPDC-E2 (lane 5) by immunoblotting. Note the epitope specificity to 2OA-PPL (lane 3) only, but not 2OA-BSA, PPL, LA-PDC and rPDC-E2. (B). This population of affinity purified antibodies were analyzed for their isotype against 2OA-PPL using anti IgM and IgG as secondary antibodies. Reactivity of affinity purified antibodies to LA-PPL and 2OA-BSA against LA-PPL and 2OA- BSA were studied in parallel. IgG was the major isotype of antibody to LA-PPL whereas IgM was the predominant isotype of antibodies to 2OA-PPL and 2OA-BSA (B). Further analysis indicated that the differences of IgG/IgM ratios among the three antibodies were statistically significant (C): IgG/IgM ratio for antibody to LA-PPL was the highest and more than 1 while the ratio for antibody against 2OA-BSA was the lowest. The ratio of the antibody to 2OA-PPL was between that of antibodies to LA-PPL and 2OA-BSA, but was significantly different from both of them. Data presented as mean ± SD. Asterisk * indicated the significant difference (****P<0.001, two-tailed unpaired t test with Welch's correction).

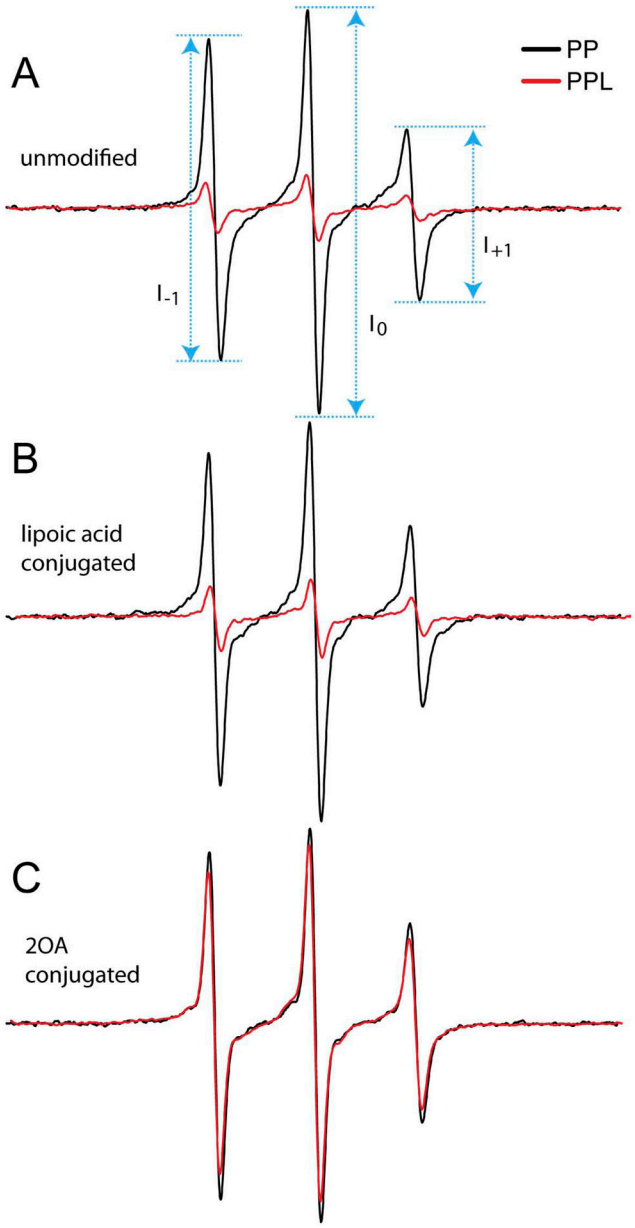

Figure 6.

Ligation induces broadening in the EPR spectra of the PPL and LA-PPL protein constructs. In panel (A), the EPR spectra of the ILD peptide (PP; black trace) is compared to the EPR spectrum of the ligated protein fragment (PPL; red trace). Line height intensities (I) used to estimate correlation times (see Methods) are indicated. Panels (B) and (C) overlay the LA- and 2OA- ILD peptides with their PDC-228 ligation products, respectively. All samples contained 30% ficoll to diminish the contribution of global rotational diffusion to the EPR line shapes. All spectra are normalized to the same molar concentration of sample as determined by protein BCA assay.

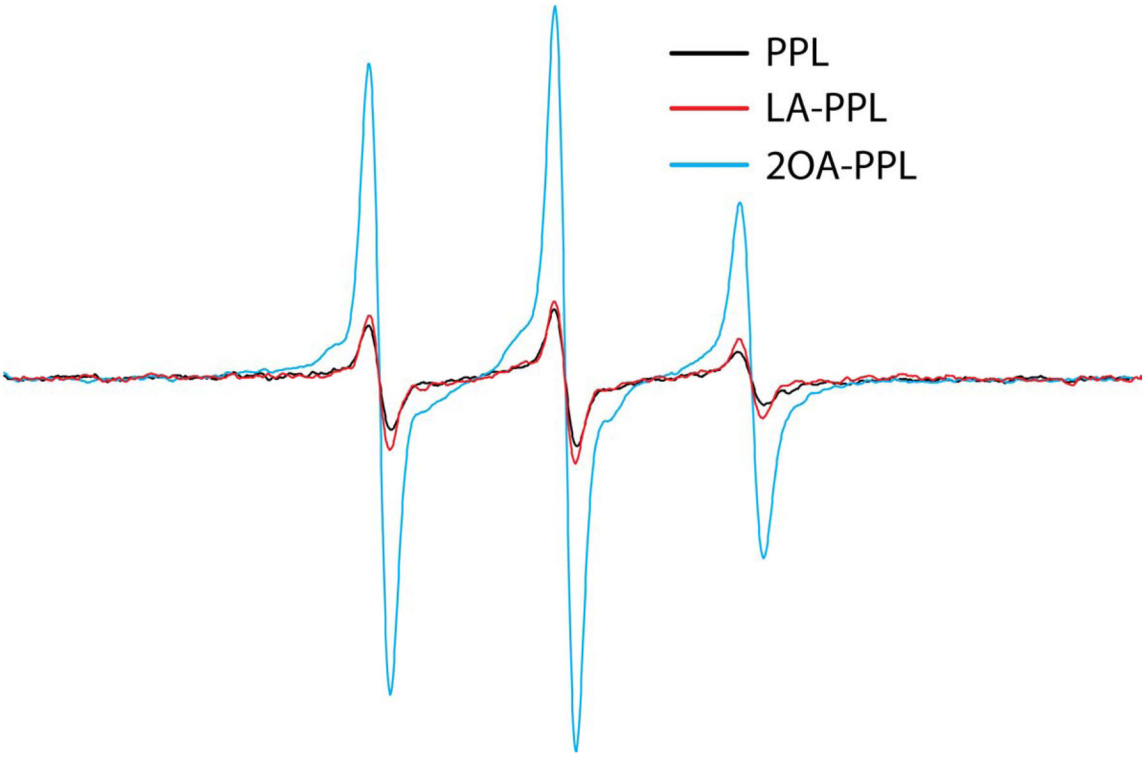

Figure 7.

Comparison of EPR spectra for the PPL ligation products (PL, LA-PPL and 2OA-PPL). All samples contained 30% ficoll to diminish the contribution of global rotational diffusion to the EPR line shapes. All spectra are normalized to the same molar concentration of sample as determined by protein BCA assay.

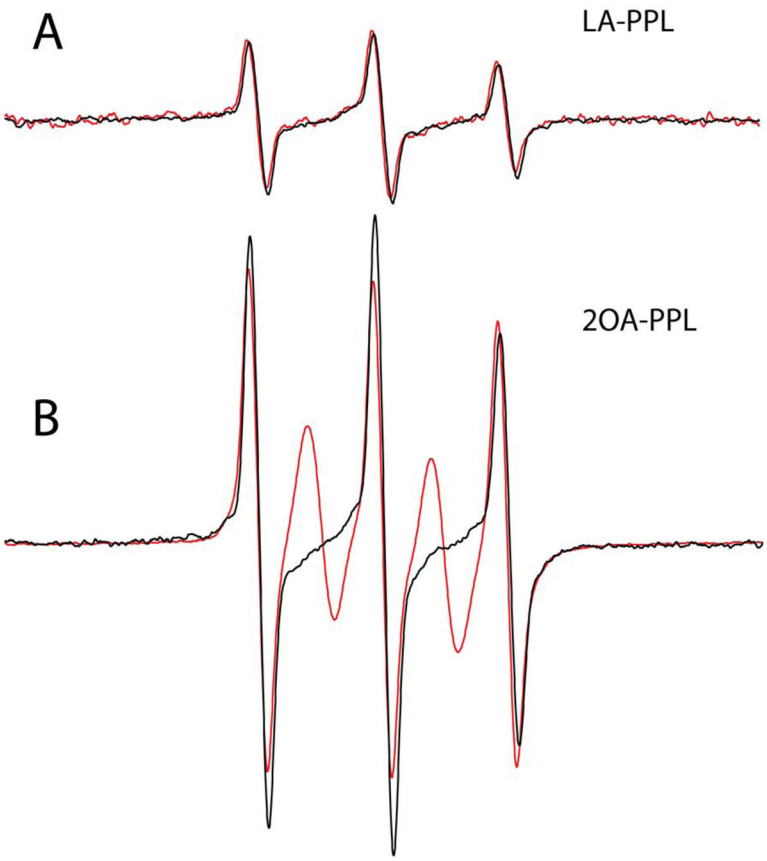

Figure 8.

Affinity purified antibodies specific to 2OA-PPL from AMA-positive sera affects the EPR spectrum of the 2OA-PPL sample, but not the LA-PPL protein construct. The EPR spectra of LA-PPL and 2OA-PPL at 1 mg/ml are shown in (A) and (B), respectively (black traces). The red traces in represent the EPR spectra following addition of the affinity antibody fraction from AMA-positive sera (final concentration of 1mg/ml) to the LA-PPL (A) and 2OA-PPL (B) samples.